Faraday Discussions

Cite this: *Faraday Discuss.*, 2014, **173**, 297

PAPER

Synthesis and first X-ray structure of a hexa-*peri*-hexabenzocoronene–fullerene-dyad: a model for an inter-carbon-allotrope hybrid†

Andreas Kratzer,[a] Jan M. Englert,‡[a] Dominik Lungerich,‡[a] Frank W. Heinemann,[b] Norbert Jux[a] and Andreas Hirsch*[a]

Received 16th April 2014, Accepted 28th May 2014
DOI: 10.1039/c4fd00069b

The synthesis of a new hexa-*peri*-hexabenzocoronene (HBC)–fullerene dyad **1** was accomplished involving a covalent linkage between both the planar and the spherical conjugated π-system of the two chromophores. We also present the first X-ray single crystal structure of a HBC–fullerene conjugate. A very short HBC–fullerene distance of 3.2 Å is observed. For the synthesis of this molecule, a new versatile applicable template, namely, a mono-functionalized hexa-*peri*-hexabenzocoronene **7** was attached to a fullerene. Absorption and fluorescence spectroscopy, as well as quantum yield measurements of **1**, indicated close electronic communication between the two subunits, which is promising for possible applications in molecular electronics.

Introduction

Hexa-*peri*-hexabenzocoronene (HBC)[1] represents a well defined D_{6h}-symmetrical substructure of graphene[2] and has recently gained increasing attention as an interesting polyaromatic hydrocarbon (PAH). The electronic and self-assembling properties of HBCs and related PAHs open a wide range of possible applications, for example, in molecular electronics. Since wet-chemical manipulations and transformations of graphene itself are still very challenging due to insolubility and difficulties in structural characterization, the investigation of suitable model compounds is highly desirable. Other remarkable and aesthetically pleasing forms of carbon are the spherical fullerenes such as their most prominent

[a]*Department of Chemistry & Pharmacy, Organic Chemistry & Interdisciplinary Center for Molecular Materials (ICMM), Friedrich-Alexander-Universität Erlangen-Nürnberg, Henkestrasse 42, 91054 Erlangen, Germany. E-mail: andreas.hirsch@chemie.uni-erlangen.de; Web: http://www.chemie.uni-erlangen.de/hirsch*

[b]*Department of Chemistry & Pharmacy, Inorganic Chemistry, Friedrich-Alexander-Universität Erlangen-Nürnberg, Egerlandstrasse 1, 91058 Erlangen, Germany*

† CCDC 997740. For crystallographic data in CIF or other electronic format see DOI: 10.1039/c4fd00069b

‡ These authors contributed equally to the work.

representative, namely, the I_h-symmetrical C_{60}. Also the fullerenes offer very promising physical properties and they have been shown to be of technological interest in solar energy conversion, drug delivery and even in cosmetics and other applications.[3]

Owing to the ability of C_{60} to accept reversibly up to six electrons,[4,5] it can be regarded as a superior electron acceptor in hybrid architectures. The systematic chemical functionalization of C_{60} allows for the combination of the outstanding fullerene properties with those of other compound classes. It can pave the way to hybrid molecules and tailor-made high performance materials.[3] For such functionalization approaches cycloaddition reactions to the [6,6]-double bonds of the fullerene core are most suitable and lead to well defined and unambiguously characterized adducts. An example is the fulleroid phenyl-C_{61}-butyric acid methyl ester (PCBM), which is still the best-performing electron acceptor component in organic photovoltaic devices.[6] Higher adducts of C_{60}, such as amphiphilic hexakis-adducts with an octahedral addition pattern exhibit superior supramolecular properties and can form shape-persistent micelles in aqueous solutions.[7] On the other hand the covalent binding of fullerenes to electroactive donor molecules such as porphyrins leads to architectures suitable for photo induced energy and/or electron transfer.[8,9]

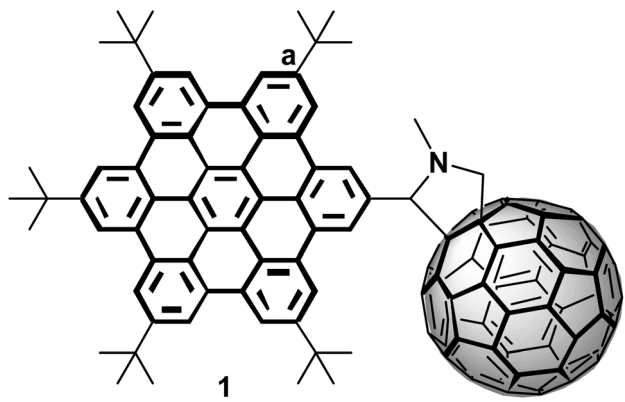

1

In previous work, targeting the PAH–fullerene interactions, assemblies resembling molecular satellite dishes that involved compounds like pyrenes or coronenes attached to heterofullerenes, had been synthesized.[10] Because it is impossible to connect isocyclic C_{60} to just one PAH by a single σ-bond, which in turn would result in radical species, a different synthetic strategy was pursued in this work allowing also for possible diversification. We report here on the synthesis, X-ray structure and physical properties of the new HBC–fullerene dyad **1**, where a planar and a spherical conjugated π-system are linked together by a bridging unit in a covalent fashion. Due to the close contact between the fullerene and the HBC core, a significant amount of mutual influence is expected. Our early investigations already showed that in a direct comparison the HBC will rather act as a donor moiety with respect to the fullerene, which is known to readily accept up to six electrons as a consequence of its triply degenerate LUMO level. These considerations are further corroborated by reports in which hexa-*peri*-hexabenzocoronene derivatives were already used as electron donating species in bulk heterojunction solar cells.[11] Furthermore, after suitable rim

functionalization, HBC can potentially act as an efficient columnar templating entity and is anticipated to allow for dynamic supramolecular self-assembly processes, which in turn will provide a new toolset for morphology control. The targeted hybrid molecule **1** represents a suitable model compound to allow direct investigation of the electronic communication between a fullerene and a hexa-*peri*-hexabenzocoronene moiety.

Results and discussion

For the chemical functionalization of fullerenes, usually wet-chemical approaches using homogeneous solutions are applied.[3] Whereas C_{60} exhibits acceptable solubility in polarizable media, the parent HBC is virtually insoluble in such solvents with some exceptions. Initial experiments using soluble hexaphenylbenzene (HPB) derivatives afforded the desired C_{60}–HPB adduct **2**, however, oxidative flattening approaches applying Scholl conditions[12] failed to supply the targeted C_{60}–HBC **3** adduct, presumably due to the very low solubility of the rigid carbon rich structure.

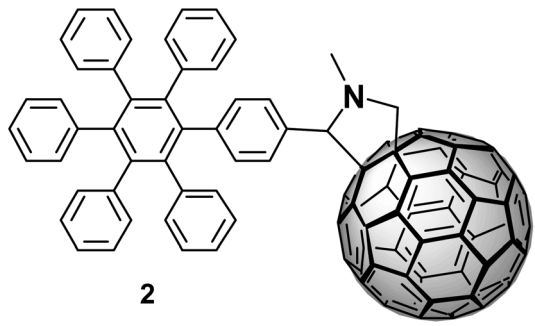

2

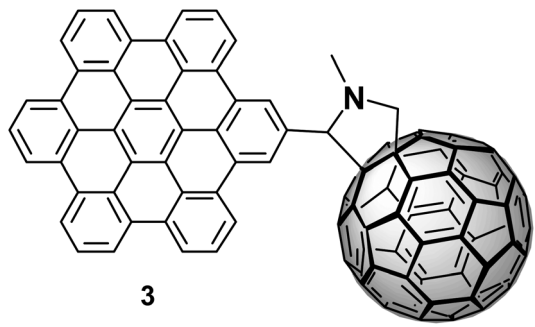

3

In order to overcome this obstacle, we had to introduce solubilizing substituents to the periphery of the HBC part. We decided to introduce solubilizing *t*-butyl groups at position **a** as identified in the representation of molecule **1**. We expected that this would provide sufficient solubility for purification and also for further processing. Accordingly, tetrakis(4-(*tert*-butyl)phenyl)cyclopenta-dienone **5** was synthesized applying a condensation reaction of 1,2-bis(4-*tert*-butylphenyl) ethane-1,2-dione and 1,3-bis(4-*tert*-butylphenyl)acetone. The dione was obtained

according to the Mueller-Westerhoff procedure[13] from 1-bromo-4-*tert*-butylbenzene, *n*-butyl lithium and 1,4-dimethylpiperazine-2,3-dione in THF in 65% yield.[14] The second building block was obtained by a two-step one-pot synthesis from 1-(bromomethyl)-4-(*tert*-butyl)benzene. After a intramolecular Claisen condensation in the first step to a β-keto ester, and a subsequent hydrolysis and decarboxylation reaction in the second step, a white powder was obtained in 86% yield.[15] In a Sonogashira reaction in toluene and triethylamine, using 4-*tert*-butyliodobenzene, $[Pd(PPh_3)_2Cl_2]$, CuI and 4-ethynyl-benzaldehyde, we synthesized the required tolane **4**.

[4 + 2] Diels–Alder cycloaddition between an appropriate tetraphenyl-cyclopentadienone derivative **5** and substituted diphenylacetylene **4** in diphenylether afforded the hexaphenylbenzene derivative **6** in 79% yield (Scheme 1). Subsequently, **6** was converted into the corresponding hexa-*peri*-hexabenzocoronene derivative **7** using an oxidative cyclodehydrogenation reaction under Scholl conditions with ferric chloride in nitromethane.[16] For this purpose 2.7 equivalents of $FeCl_3$ per to be formed C–C-bond were pre-dissolved in dry $MeNO_2$ and ice cooled CH_2Cl_2 [12] to obtain **7** in an oxidative flattening progress in quantitative yield. Purification was accomplished by recrystallization from $CHCl_3$ and MeOH or by flash chromatography (DCM–hexanes 1 : 1), if necessary. The confirmation of the successful planarization from **6** to **7** was provided by ^{1}H NMR spectroscopy. Only the expected ten magnetically inequivalent sets of protons were detected. The exact mass of **7** was recorded by ESI-HR spectrometry, where the corresponding M^+ signal was detected at 830.44. In addition, the appearance of the expanded HBC chromophore was confirmed by UV/vis absorption spectroscopy.

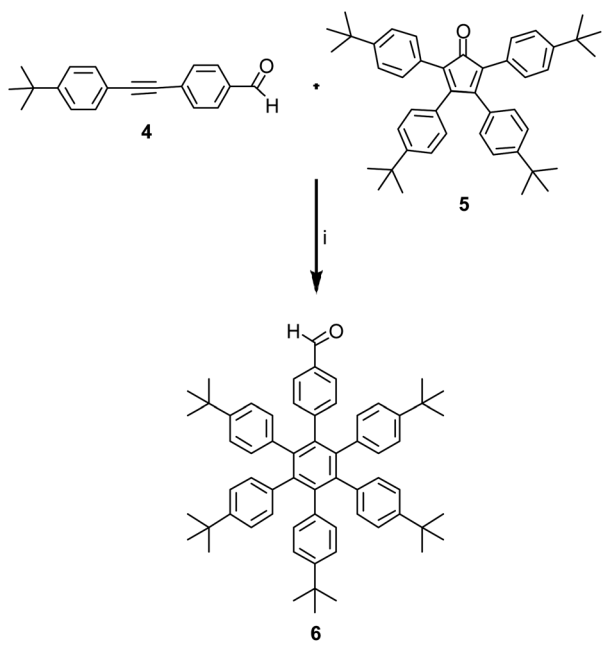

Scheme 1 Synthesis of the formyl-substituted hexaphenylbenzene **6**. (i) Diphenylether, reflux (79%).

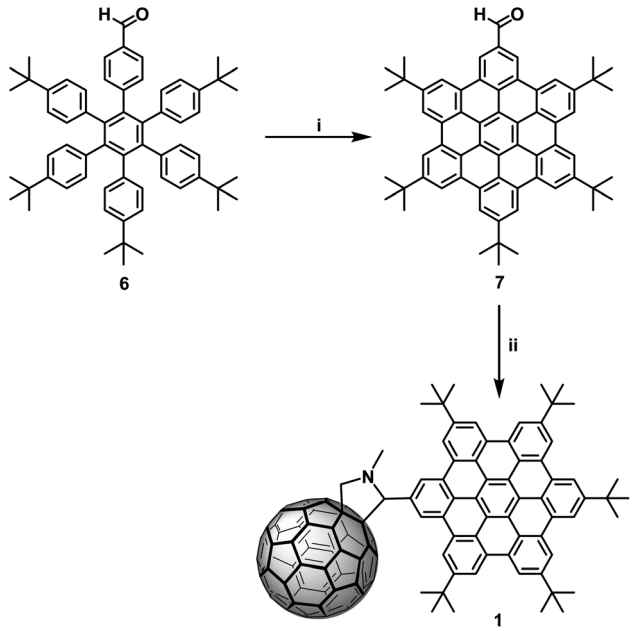

Scheme 2 (i) 16 equiv. dry $FeCl_3$–$MeNO_2$ (300 mg mL^{-1}), CH_2Cl_2, 0 °C, 2.5 h; (ii) 1.2 equiv. C_{60}, 1.2 equiv. sarcosine, toluene, reflux, overnight.

In a final [3 + 2] dipolar cycloaddition, the HBC aldehyde **7**, sarcosine and C_{60} were reacted in refluxing toluene to form the intermediate HBC ylide, which underwent a mono-addition to a [6,6]double bond of the fullerene to give the target molecule **1**. Purification was carried out by flash chromatography (toluene–hexanes 7 : 3) to give **1** as a racemate in a good yield of 79%. The resulting brownish solid was dissolved in CH_2Cl_2 and precipitated with *n*-pentane to minimize solvent inclusions. Characterization by ^{1}H NMR provided evidence for the successful reaction (Scheme 2).

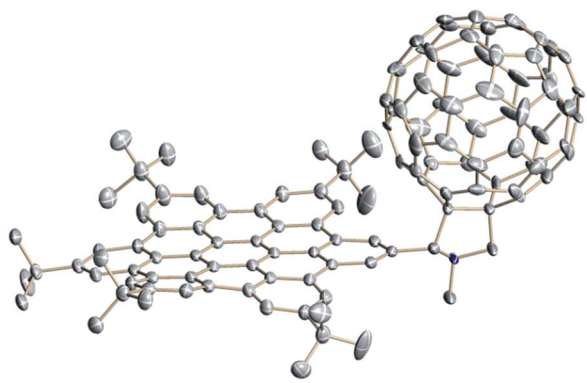

Fig. 1 Thermal ellipsoid representation of the molecular structure of (*R*)-**1** of (*R*/*S*)-**1** in the solid state crystal structure (50% probability ellipsoids; hydrogen atoms, disorder and solvent molecules omitted for clarity).

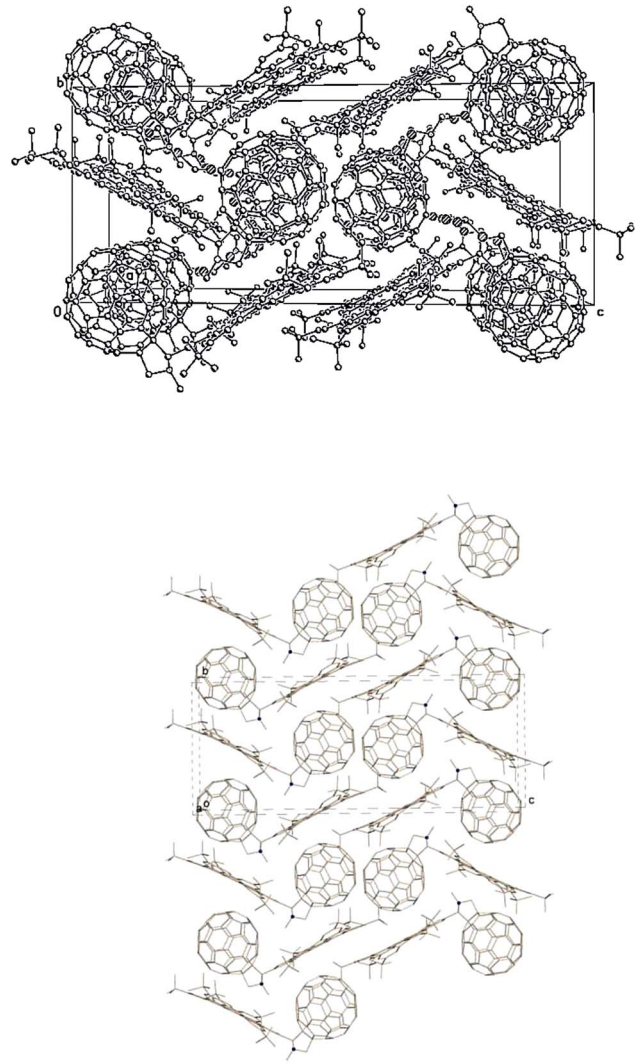

Fig. 2 Crystal packing of the HBC–fullerene hybrid **1**. For reasons of clarity the arrangement of (*R*/*S*)-**1** in the crystal is represented as homochiral strands.

The peaks for the two diastereotopic pyrolidine protons appear as two doublets at 4.24 and 4.94 ppm with a coupling constant of 9.66 Hz. The methyl group at the N-atom is recorded as a singlet at 2.85 ppm. The signal for the aldehyde vanished due to the functionalization with C_{60}. The ^{13}C NMR also confirmed the structure of **1**. The stereogenic carbon center is identified by the signal at 84.2 ppm, the carbon atom of the methyl group at the nitrogen atom likewise resonates at 40.0 ppm. The carbon atom, where the two diasterotopic protons are located, resonates at 68.9 ppm, the signals for the sp^3-hybridized carbon atoms at the fullerene are observed at 68.9 and 69.9 ppm. The typical sp^2-C_{60} signals are detected in the specific region for a monoadduct between 134.7 and 155.9 ppm. The successful formation of **1** was also confirmed by ESI-TOF HR-mass spectrometry and the

exact molecular weight was measured as $m/z = 1577.49$. UV/vis absorption spectroscopy indicated the typical HBC bands at 346, 362 and 392, as well as the typical feature for a fullerene monoadduct at 431 nm.[3]

To obtain a better insight into the crystal packing and supramolecular interaction between the two molecular entities, X-ray crystallography was applied.[17] Single crystals of **1** were grown by slow vapor diffusion of pentane into a chloroform solution of compound **1**, which subsequently crystallized as a racemic mixture in the achiral monoclinic space group $P2_1/n$ and contains four molecules of $CHCl_3$ in the asymmetric unit of the unit cell. We want to emphasise in this context, that this is the first reported crystal structure of a hexa-*peri*-hexabenzocoronene–fullerene hybrid (Fig. 1). Due to the statistic arrangement of both (*R*)-**1** and (*S*)-**1** in the crystal, the data set was refined in such a way that (*R*)-**1** and (*S*)-**1** appear as a superposition of each in the asymmetric unit with a distribution of 51.6% and 48.4%. The monomers in the crystal form one-dimensional strands of (*R*/*S*)-**1** with the said distribution, which is inverted in half of the strand due to a center of inversion in the crystal. Some structural features of the crystal structure of **1** are especially noteworthy. There are two interesting π–π-

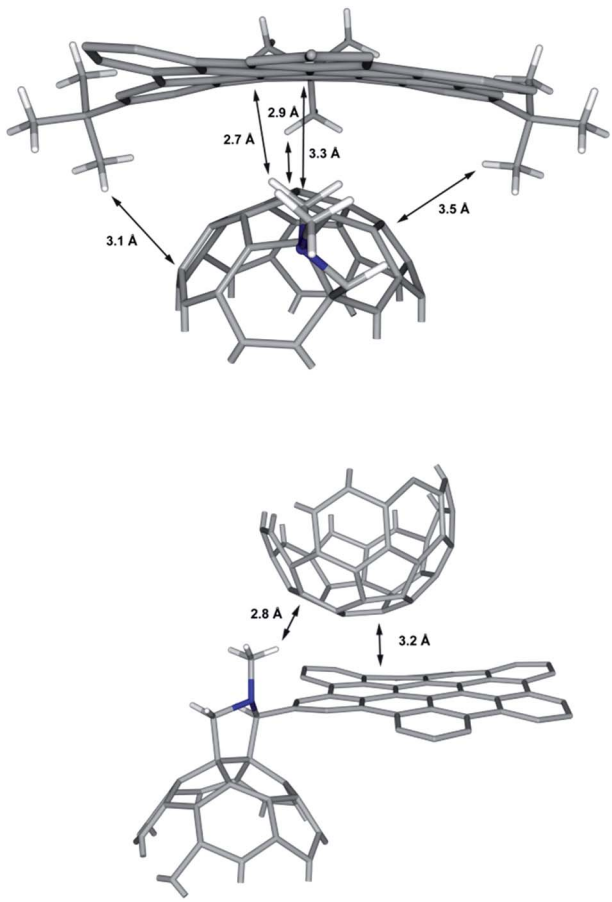

Fig. 3 Distances in the close contact HBC–fullerene hybrid **1**.

interactions between the HBC and the fullerene within the crystal packing. The shortest measured sp^2–sp^2-distance between the HBC and the neighbouring fullerene cage is 3.2 Å (Fig. 2) and hence shorter than the distance between two single layers in graphite, which is 3.35 Å.[18] The planar HBC geometry is distorted to accommodate the ball-shaped structure of the fullerene and maximize π–π-interactions between the fullerene and the HBC moiety, as well as the C–H/π-interactions between the *t*-butyl-groups and the fullerene cage.

All these interactions lead to a close contact crystal packing. There are further very short distances within the hybrid material. The methyl group at the nitrogen atom has a distance of only 2.8 Å to the fullerene cage (Fig. 2), the H atoms of the *t*-butyl groups are around 3.3 Å away from the C_{60} moiety. The shortest distance between two fragments, namely one diastereotopic proton at the methylene bridge to the nitrogen atom and the HBC plane, was measured to be around 2.7 Å (Fig. 3).

Furthermore, fundamental photo physical properties of the novel hybrid material were investigated. The presence of HBC was determined by its characteristic absorption/emission spectroscopy of **1** (Fig. 4). The most intense HBC p-band transition of **1** is observed at $\lambda_{max} = 361$ nm.

The extinction coefficient was obtained by fitting the absorbance against the concentration in agreement with Beer's law. Dyad **1** exhibits an extinction coefficient of 200 000 M^{-1} cm^{-1}. Compared to known HBC derivatives the extinction coefficient is relatively high. Functionalized fullerenes, in which chromophores or electroactive moieties are covalently linked to the fullerene cage, offer distinct advantages such as molecular extinction in the visible region of the spectrum, the preference for a population of singlet *versus* triplet excited states and the ultimate fates (*i.e.*, lifetimes and reactivity) of these excited states.[19] This makes hybrid **1** a candidate for applications in bulk heterojunction solar cells. Ongoing studies will clarify if the effect arises from the fullerene moiety. Fluorescence quantum yields of synthesized compounds **1** and **7** were determined by a standard literature procedure using anthracene as a reference standard ($\Phi = 0.33$ in THF).[20] We observed a quantum yield of 12.3% for the HBC–CHO precursor **7**, whereas the

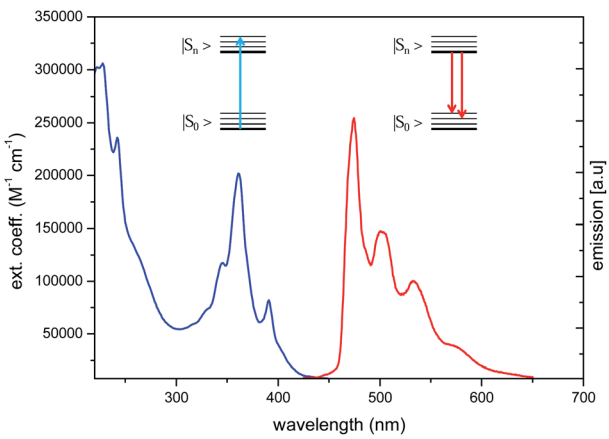

Fig. 4 Absorption/emission spectra of **1**.

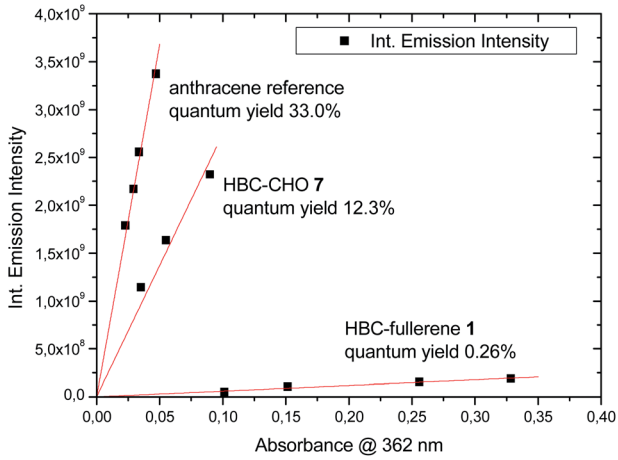

Fig. 5 Quantum yield of anthracene reference, HBC–CHO **7** and HBC–fullerene **1**.

quantum yield of the hybrid material was determined to be as low as 0.26% (Fig. 5). These results indicate strong electronic interaction between the HBC moiety and the fullerene. The quenching of the HBC like emission is explained by

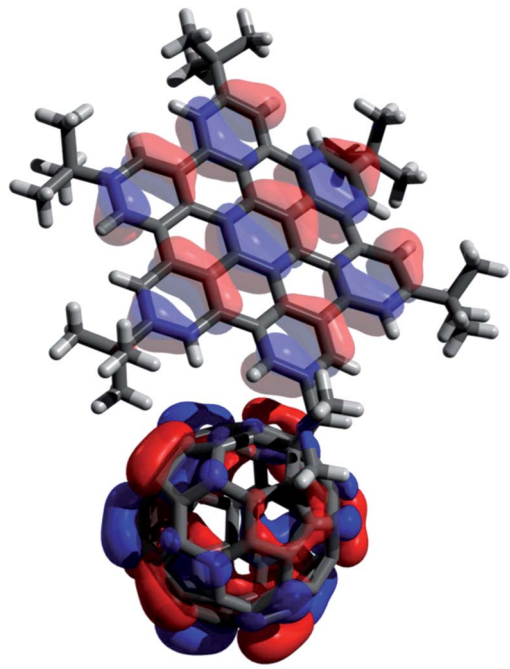

Fig. 6 Molecular orbital (MO) representation of the fullerene–HBC dyad (**1**) on a DFT B3LYP/6-311G quantum mechanical level of theory as calculated using Gaussian '09. The HOMO (translucent) is centered on the HBC unit while the LUMO (solid) is exclusively located on the fullerene cage.

Table 1 Half-wave potentials, HOMO and LUMO energy levels and band gap energy of hybrid **1**.[21]

$E_{1/2(red1)}$	$E_{1/2(red2)}$	$E_{1/2(red3)}$	$E_{1/2(red4)}$	$E_{1/2(ox1)}$	E_{HOMO}	E_{LUMO}	E_{gap}
−0.95	−1.35	−1.50	−1.90	1.18	−6.0	−3.9	2.1

strong electronic communication between both – fullerene and HBC – moieties. We have to note though, that an additional reduction of the fluorescence quantum yield is expected due to the presence of the nitrogen lone pair in the pyrolidine ring.

DFT calculations gave good evidence for the location of the LUMO on the fullerene, while the HOMO is centered round the HBC (Fig. 6). We applied cyclic voltammetry to investigate the electrochemical properties of **1** (Table 1). Four reversible reduction processes and one reversible oxidation process were observed. The first half-wave reduction potential is about −0.95 eV, the first half-wave oxidation potential around 1.18 eV, resulting in a HOMO energy level of −6.0 eV and a LUMO energy level of −3.9 eV. For an efficient charge transfer, *e.g.* in polymer solar cells, from the donor to the acceptor fullerene, the relative position of donor LUMO and the acceptor LUMO is crucial.

Compared to PCBM ($E_{HOMO} = -6.1$ eV, $E_{LUMO} = -3.7$ eV),[22] the LUMO energy of **1** is around 0.2 eV lower. Also the HOMO–LUMO gap is lower by −0.3 eV, however, these energy differences are rather small. The PM3 calculated differences of the LUMO energies (HyperChem) of PCBM and **1** are $\Delta E_{LUMO} = 0.07$ eV. This corroborates the experimental results. Both, B3LYP/6-311G and PM3 calculations clearly show that the HOMO of **1** is HBC-centered. The calculated HOMO energies are significantly above the occupied orbital levels of the C_{60} core. As a consequence a comparison between the HOMO–LUMO gap of PCBM and **1** is not suitable.

Conclusion and outlook

In this contribution we have presented the synthesis of a HBC–fullerene hybrid molecule with a covalent linkage between both moieties. For this purpose we have synthesized a new hexa-*peri*-hexabenzocoronene compound, which could serve as a versatile template for optoelectronic applications. Furthermore, we presented the first X-ray crystal structure of a HBC–fullerene hybrid molecule, where a very close contact of 3.17 Å between the two aromatic units was observed. Besides the synthesis and the structure determination, optical and electronic properties were investigated. Steady-state emission spectroscopies and determination of the extinction coefficient as well as quantum yield measurements provide evidence for close electronic communication between the two entities in the dyad. A detailed investigation of possible electron or energy transfer processes in this dyad and related yet to be synthesized systems will be a topic of future research in our laboratories. In this work HBC was implemented to serve as a model compound to assess fundamental structural and photophysical properties of such assemblies. Detailed time resolved spectroscopic investigations, which are expected to allow in depth characterization of the underlying photophysics, will

provide a more detailed picture of the roles of the HBC entity as well as its effect on the fullerene acceptor. Concerning the results of previous works,[10] as well as our initial investigations presented in this paper, nearly quantitative transduction of photoexcited states to the rigidly linked buckyball can be anticipated. Also, further functionalization of this hybrid material to yield fullerene hexakis-adducts is currently underway. Such architectures could even provide water solubility. Furthermore, HBC–fullerene hybrids will be tested as self-sensitized acceptor materials in bulk heterojunction organic solar cells.

Experimental section

General remarks and chemicals

Chemicals were purchased from commercial sources and were used without further purification (unless otherwise stated). C_{60} was purchased from IoLiTec Nanomaterials. Solvents were distilled before use; solvents that generated acid had K_2CO_3 in the distillation flask. For reactions with fullerenes, HPLC grade solvents were used. TLC: Merck TLC silica gel 60 F254. UV/vis spectroscopy: Perkin Elmer Lambda 1050, THF as solvent, absorption maxima given in nm, extinction coefficients given in M^{-1} cm^{-1}. IR spectroscopy: attenuated total reflectance (ATR), Bruker FTIR Tensor 27 instrument. NMR spectroscopy: Bruker Avance 400 or Avance 300 spectrometer. Field strengths are given as the resonance frequency of the respective nuclei. The chemical shifts are given in ppm relative to tetramethylsilane (TMS). Abbreviations: s singlet, d doublet, m multiplet, br broad. Spectra were recorded at room temperature. MALDI MS: Shimadzu Axima Confidence instrument (TOF). ESI MS: Bruker Daltronics micrOTOF (TOF) instrument. Matrices: (*E*)-2-(3-(4-(*tert*-butyl)-phenyl)-2-methyl allylidene) malononitrile (dctb), 3,5-dimethoxy-4-hydroxycinnamic acid (sin).

4-((4-(*tert*-Butyl)phenyl)ethynyl)benzaldehyde (4). 4-*tert*-Butyliodobenzene (250 mg, 0.96 mmol, 1.0 equiv.), $[Pd(PPh_3)_2Cl_2]$ (13 mg, 0.02 mmol, 0.2 equiv.), and CuI (7 mg, 0.04 mmol, 0.02 equiv.) were dissolved in dry toluene (5 mL) and triethylamine (5 mL) under an argon atmosphere. Subsequently 4-ethynylbenzaldehyde (150 mg, 1.15 mmol, 1.2 equiv.) was added at once and the mixture was stirred overnight. After filtration the solvent was removed, and the crude mixture was purified by flash chromatography (SiO_2, toluene). The product was obtained as a pale yellow solid (195 mg, 77%).

^{1}H NMR (400 MHz, $CDCl_3$): δ [ppm] = 1.32 (s, 9H), 7.37–7.39 (m, 2H), 7.46–7.49 (m, 2H), 7.64–7.66 (m, 2H), 7.83–7.85 (m, 2H).

^{13}C NMR (100.5 MHz, $CDCl_3$): δ [ppm] = 31.1, 34.9, 88.0, 93.8, 119.4, 125.5, 129.6, 129.9, 131.5, 132.0, 135.2, 152.4, 191.4.

MS (MALDI, sin): *m*/*z*: 262 [M^+].

IR (ATR, diamond): $\tilde{\nu}$ [cm^{-1}] = 2964, 2867, 2826, 2726, 1696, 1597, 1560, 1362, 1203, 1103, 829, 813.

HPB–CHO (6). Compound **2** (129 mg, 0.49 mmol, 1.0 equiv.) and cyclopentadienone **5** (300 mg, 0.49 mmol, 1.0 equiv.) were dissolved in diphenylether (2.5 mL) and refluxed at 270 °C overnight. After the mixture was allowed to cool to room temperature, methanol was added. The precipitate was filtered and washed several times with cold methanol. The product was obtained as a grey solid (249 mg, 60%).

^{1}H NMR (300 MHz, $CDCl_3$): δ [ppm] = 1.08 (s, 45H), 6.65 (m, 10H), 6.80 (m, 10H), 7.02 (m, 2H), 7.35 (m, 2H), 9.73 (s, 1H).

^{13}C NMR (100.5 MHz, $CDCl_3$): δ [ppm] = 31.2, 34.0, 3421, 123.1, 123.4, 128.0, 130.9, 131.0, 132.3, 133.1, 137.3, 137.5, 137.6, 138.5, 139.8, 140.8, 141.2, 147.5, 147.6, 148.0, 148.5, 192.4.

MS (MALDI, sin): m/z = 842 [M^+].

HRMS (ESI, MeCN–toluene): calcd for $C_{63}H_{70}O^+$ [M^+]: 842.54266, found: 842.54289.

IR (ATR, diamond): $\tilde{\nu}$ [cm^{-1}] = 2961, 2903, 2866, 1705, 1602, 1392, 1361, 1206, 1018, 861, 832.

HBC–CHO (7). To an ice-cooled, argon-saturated solution of **6** (100 mg, 0.12 mmol, 1.0 equiv.) in 50 mL dry dichloromethane, a freshly prepared solution of anhydrous $FeCl_3$ (352 mg, 2.16 mmol, 18 equiv.) in dry nitromethane (5.0 mL) was added dropwise by syringe through a pressure equilibrated septum while maintaining a low but constant stream of argon passing through the solution. Cooling was maintained for typically one hour and the evaporated solvent was replaced if necessary. Subsequently, the flask was sealed and stirred for 8 hours. Afterwards the reaction was quenched by the addition of 50 mL cold methanol. The resulting mixture was filtered and purified by recrystallization from $CHCl_3$ (10 mL) and methanol (10 mL). Further purification could be performed by column chromatography (silica gel, DCM–hexanes 1 : 1), if necessary. The final product was obtained as a yellow solid in good to quantitative yields.

^{1}H NMR (400 MHz, $CDCl_3$): δ [ppm] = 1.69 (s, 18H), 1.86 (s, 18H), 1.90 (s, 9H), 8.69 (m, 2H), 8.81 (m, 2H), 8.93 (m, 2H), 9.06 (m, 2H), 9.19 (m, 2H), 9.24 (m, 2H), 10.17 (s, 1H).

^{13}C NMR (100.5 MHz, $CDCl_3$): δ [ppm] = 32.0, 32.1, 35.6, 35.7, 35.8, 118.7, 118.8, 118.9, 119.0, 120.0, 120.8, 121.2, 121.5, 123.1, 123.3, 123.4, 128.7, 129.1, 129.8, 129.9, 130.1, 130.3, 130.5, 132.6, 148.6, 148.8, 149.2, 192.5.

MS (MALDI, om): m/z = 831 [M^+].

HRMS (ESI, MeCN–CH_3Cl): calcd for $C_{63}H_{58}O^+$ [M^+]: 830.44876, found 830.44928.

IR (ATR, diamond): $\tilde{\nu}$ [cm^{-1}] = 2954, 2923, 2854, 1697, 1607, 1367, 1184, 867.

UV/vis (THF): λ_{max}: 333, 349, 369, 400, 423, 447, 476 nm.

HBC–fullerene (1). Compound **7** (50 mg, 0.60 mmol, 1.0 equiv.) was dissolved in toluene (50 mL) under inert conditions before C_{60} (52 mg, 0.07 mmol, 1.2 equiv.) was added. The mixture was stirred for 30 minutes under exclusion of light until C_{60} was dissolved completely. Then sarcosine (6.0 mg, 0.07 mmol, 1.2 equiv.) was added and the mixture was refluxed overnight. After cooling down to room temperature and filtration the crude mixture was purified by flash chromatography (SiO_2, toluene–hexanes 7 : 3). The occurring brown solid was dissolved in CH_2Cl_2 and precipitated with *n*-pentane to exclude solvent inclusions (70 mg, 66%).

^{1}H NMR (400 MHz, $CDCl_3$): δ [ppm] = 1.79 (s, 18H), 1.81 (s, 27H), 2.85 (s, 3H), 4.24 (d, 1H, ^{2}J = 9.66 Hz), 4.93 (d, 1H, ^{2}J = 9.66 Hz), 5.46 (s, 1H), 9.26 (s, 2H), 9.29 (s, 2H), 9.30 (s, 6H), 9.57 (s, 2H, br).

^{13}C NMR (100.5 MHz, $CDCl_3$): δ [ppm] = 29.8, 31.7, 31.7, 32.0, 35.1, 35.2, 40.0, 68.9, 69.9, 84.3, 118.8, 118.8, 119.1, 119.2, 120.0, 120.3, 120.5, 120.7, 122.7, 123.6, 123.7, 123.7, 125.9, 129.9, 130.1, 130.2, 130.3, 130.8, 134.7, 135.4, 135.6, 135.9, 136.2, 141.1, 141.3, 141.3, 141.4, 141.5, 141.6, 141.6, 141.7, 141.9, 142.0, 142.0, 142.1, 142.2, 142.3, 142.6, 142.8, 144.0, 144.2, 144.3, 144.7, 144.7, 144.8, 145.1,

145.1, 145.1, 145.2, 145.2, 145.3, 145.3, 145.4, 145.5, 145.7, 145.7, 145.8, 145.9, 146.0, 146.2, 146.8, 146.8, 148.3, 148.4, 148.6, 153.0, 153.4, 153.5, 155.9.

MS (MALDI, dctb): $m/z = 1578$ [M^+].

HRMS (ESI, MeCN–$CHCl_3$): calcd for $C_{122}H_{65}O_3^+$ [M^+]: 1577.49828, found: 1577.49089.

IR (ATR, diamond): $\tilde{\nu}$ [cm^{-1}] = 2952, 2921, 2852, 1731, 1606, 1579, 1461, 1362, 1259, 868.

UV/vis (THF): λ_{max} (ε, M^{-1} cm^{-1}): 330 (73 000), 345 (117 000), 361 (202 000), 391 (82 000), 431 (10 000) nm.

Acknowledgements

The authors thank the Deutsche Forschungsgemeinschaft (DFG-SFB 953 "Synthetic Carbon Allotropes", Projects A1 and A2) and the Bayrisches Staatsministerium für Bildung und Kultus, Wissenschaft und Kunst ("Solar Technologies Go Hybrid", SolTech; Energiecampus Nürnberg, EnCN) for financial support.

References

1 J. Wu, W. Pisula and K. Müllen, *Chem. Rev.*, 2007, **107**, 718.
2 A. K. Geim and K. S. Novoselov, *Nat. Mater.*, 2007, **6**, 183.
3 A. Hirsch, M. Brettreich and F. Wudl, *Fullerenes: Chemistry and Reactions*, Wiley, 2006.
4 L. Echegoyen and L. E. Echegoyen, *Acc. Chem. Res.*, 1998, **31**, 593.
5 Q. Xie, E. Perez-Cordero and L. Echegoyen, *J. Am. Chem. Soc.*, 1992, **114**, 3978.
6 J. C. Hummelen, B. W. Knight, F. LePeq, F. Wudl, J. Yao and C. L. Wilkins, *J. Org. Chem.*, 1995, **60**, 532.
7 S. Burghardt, A. Hirsch, B. Schade, K. Ludwig and C. Böttcher, *Angew. Chem.*, 2005, **117**, 3036.
8 D. M. Guldi, *Chem. Soc. Rev.*, 2002, **31**, 22.
9 H. Imahori and Y. Sakata, *Adv. Mater.*, 1997, **9**, 537.
10 F. Hauke, S. Atalick, D. M. Guldi, J. Mack, L. T. Scott and A. Hirsch, *Chem. Commun.*, 2004, 766.
11 S. J. Kang, S. Ahn, J. B. Kim, C. Schenck, A. M. Hiszpanski, S. Oh, T. Schiros, Y.-L. Loo and C. Nuckolls, *J. Am. Chem. Soc.*, 2013, **135**, 2207.
12 S. P. Brown, I. Schnell, J. D. Brand, K. Müllen and H. W. Spiess, *J. Am. Chem. Soc.*, 1999, **121**, 6712.
13 U. T. Mueller-Westerhoff and M. Zhou, *J. Org. Chem.*, 1994, **59**, 4988.
14 A. Gourdon, S. K. Sadhukhan and C. Viala, *Synthesis*, 2003, 1521.
15 D. Romer, *Synthesis*, 2011, **2011**, 2721.
16 J. M. Englert, J. Malig, V. A. Zamolo, A. Hirsch and N. Jux, *Chem. Commun.*, 2013, **49**, 4827.
17 ESI.†
18 H. Marsh and F. Rodríguez-Reinoso, *Sciences of carbon materials*, Universidad de Alicante, 2000.
19 D. M. Guldi and N. Martin, *Fullerenes: From Synthesis to Optoelectronic Properties*, Springer, 2003.
20 S. L. Murov, I. Carmichael and G. L. Hug, *Handbook of Photochemistry*, Taylor & Francis, 2nd edn, 1993.

21 T. P. I. Saragi, T. Spehr, A. Siebert, T. Fuhrmann-Lieker and J. Salbeck, *Chem. Rev.*, 2007, **107**, 1011.
22 C. Brabec, U. Scherf and V. Dyakonov, *Organic Photovoltaics: Materials, Device Physics, and Manufacturing Technologies*, Wiley, 2011.

